A Novel Approach for Development of Neural Network based Electrical Machine Models for HEV System-level Design Optimization

Christian Gletter[1], Andre Mayer[1], Josef Kallo[2], Thomas Winsel[3] and Oliver Nelles[4]

[1]*Daimler AG, Stuttgart, Germany*

[2]*Faculty of Engineering, Computer Sciences and Psychology, Ulm University, Germany*

[3]*Department of Mechanical Engineering, Kempten University of Applied Sciences, Germany*

[4]*Department of Mechanical Engineering, University of Siegen, Germany*

Abstract: To find the optimal system-level design of hybrid electric vehicles (HEVs), component models are used in simulations to evaluate a large number of different designs within a high dimensional design space. As the electrical machine (EM) represents a key component of the HEV powertrain in terms of energy consumption, models require scalability and sufficient accuracy with manageable computational effort. This paper presents a novel approach for the development of scalable EM models based on Neural Networks (NN). The models are trained with data derived by a Finite Element Analysis (FEA) based scaling procedure and capable to represent the characteristics of a wide range of EM designs without the incorporation of further details. Once a model is trained, it can be directly used in system-level design optimization. The practicality of the model is proven within an exemplary simulation study and its goodness of fit to the training data is validated by a statistical analysis. This approach can help to reduce the computational effort of EM efficiency maps calculation, since only a small number of time-consuming FEA based scaling simulations must be performed prior to the optimization.

1 INTRODUCTION

Since the system-level design of HEVs considers different topologies, technologies and component sizes as well as control strategies, the optimization of such systems becomes a challenging task. Therefore, research has been done on optimal control strategies (Wirasingha and Emadi, 2011), component sizing (Gao and Porandla, 2005) and topology optimization (Hofman et al., 2012). Within the latest publications, optimization-based frameworks are being developed to consider two or more system levels within the optimization problem (Silvas et al., 2016). Thus, the number of design variables and therefore the number of evaluations for HEV designs increases. Since simulation models are used for the evaluation of different HEV designs, appropriate component models, e.g., the electrical machine as a key component of HEV powertrain, must be scalable with corresponding design variables while satisfying accuracy and computational effort requirements.

In system-level design optimization the axial and radial dimensions and/or the number of turns per coil are often used for sizing the EM. Therefore, so called scaling laws are suitable to describe the functional relationship between a change in the design variable and its effect on the EM characteristics within specific limitations (e.g., same basic construction). In (Buecherl et al., 2010) analytical models based on equivalent circuits of different types of EMs are developed. The axial and radial scaling is expressed by scalar factors, which are applied within scaling laws to represent the influence on the equivalent circuit's elements such as resistances (losses) and inductances and thus the EM characteristics. Analytical scaling laws are also applied in the method presented in (Stipetic and Goss, 2016), where a saturated flux-linkage model and loss model are used to determine the characteristics of a reference electrical machine. Here, the winding is considered as additional design variable and incorporated by a specific scaling factor.

Another approach is the use of existing efficiency maps as baseline models and applying scaling methods to adapt the characteristics of the component

17

within an appropriate design range. The baseline efficiency maps are obtained by measurement data or highly accurate but time-consuming modeling approaches such as Finite Element Analysis (FEA). In (Zhou et al., 2015), a database which represents basic EM characteristics over a wide design range, is obtained by FEA. The baseline design is then scaled by means of dimensional quantities and the number of turns per coil to generate new EM designs. A similar approach is presented in (Domingues et al., 2016), where a database represents EMs separated by the categories constant power speed range (CPSR) and outer radius. The efficiency maps of new machine designs are then calculated by applying a linear axial scaling law to specific electrical machine losses.

(Vaillant, 2016) proposes an interesting scaling method based on data representing combined efficiency maps of EM and power electronics (PE) and thus the EM system. The baseline designs are categorized into classes of EM systems with different axial dimensions and therefore different power levels. In order to calculate new efficiency maps, a regression function is fitted to a data set consisting of one normalized speed-torque combination for each baseline map within one class. Repeating this step for each speed-torque combination allows one to scale the efficiency maps by varying the power of the EM system.

In order to allow the development of data based efficiency models without explicit consideration of scaling laws and presorting different machine designs into specific classes, a powerful nonlinear regression method is required. Since specific types of Neural Networks are known as universal approximators (Hornik et al., 1989) and thus are capable of modeling complex nonlinear system behavior, this paper presents a novel approach for the development of scalable efficiency models based on NNs for the use in system-level design optimization.

2 NEURAL NETWORKS

The idea of NN is originally motivated by the replication of powerful structure of biological neural networks for tasks such as information processing, learning and adaptation (Nelles, 2001). Thus, NNs are well suited to learn and adapt system behavior from data of the process within the system i.e the functional relationship between the input and output variables.

2.1 Multilayer Perceptron

The exemplary network structure of a multilayer perceptron (MLP) is shown in Figure 1 since this type of

NN is used in this work. It consists of one input layer, one hidden layer and one output layer, and therefore represents a three layer network. The mathematical expression for this single output network is given by

$$\hat{y} = b^{(2)} + \sum_{i=1}^{N_n} w_i^{(2)} \sigma \left[b_i^{(1)} + \sum_{j=1}^{N_u} w_{i,j}^{(1)} u_j \right], \quad (1)$$

where N_n denotes the total number of neurons i within the hidden layer and N_u the number of inputs u_j. The weights and biases, which are optimized by a training algorithm, are denoted by w and b, respectively. The superscripts (1) and (2) refer to the corresponding layer (hidden and output layer).
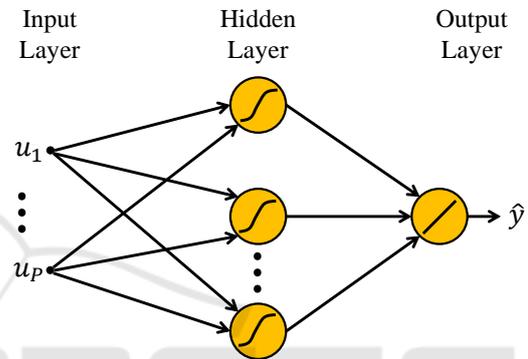

Figure 1: Structure of a three layer perceptron.

The nonlinear nature of the MLP arises through one-dimensional so-called activation functions σ. A common choice of activation function is the hyperbolic tangent (tanh), which is also used in this work.

2.2 Training of Multilayer Perceptrons

In general, the adaption of a model in order to represent a process behavior is known as system identification (Nelles, 2001).
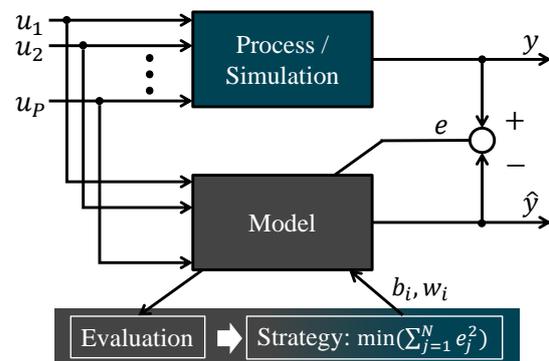

Figure 2: Schematic of system identification process, modified (Nelles, 2001).

Figure 2 illustrates the system identification schematically. An optimization procedure varies the biases and the weights of the MLP in both layers, while the model is fed with the same inputs as the process. The optimization goal is to minimize the model error e given by the difference of the process output y and the model output $\hat{y}$. The block diagram in the figure suggests an online optimization procedure. In this work, the training for the MLP is carried out offline and thus is based on a data set consisting of previously gathered data points within the design space, i.e different combinations of values of the input variables $\underline{u} = [u_1, u_2, \ldots, u_{N_u}]^T$, and its corresponding output values y. The values y for each input combination u may be drawn either from measurements of the real process or from complex simulation models. In the literature, different algorithms have been used for the training of MLPs, where the most common one is the backpropagation algorithm. Since this paper focuses on a novel approach for the application of MLPs in the development of scalable efficiency models of electrical machines, the well-known training algorithms will not be discussed in detail. However, for further details on backpropagation algorithm the reader may refer to (Rumelhart et al., 1986).

3 METHODICAL APPROACH

Based on the theoretical background of Multilayer Perceptrons and model training, the methodical approach for the development MLP-based scalable EM models (SEMMs) is explained within this section. An overview of the approach is shown schematically in Figure 3.
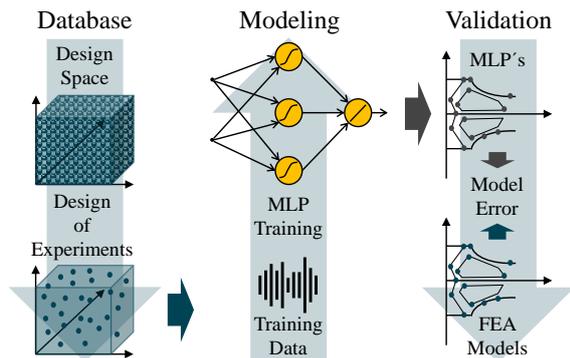

Figure 3: Schematic of the methodical approach for development of MLP-based scalable EM models.

Starting from the left top, a wide range of different electrical machines are described within the design space. The term design describes a specific electrical machine characterized by its corresponding design

variables. In order to reduce the computational effort, a design of experiments (DoE) approach is applied, which leads to the corresponding training data for the MLP training illustrated in the middle of the figure. Subsequent to the training procedure, the accuracy of the MLP-based scalable EM model is assessed by comparison with highly accurate FEA based models. In the following, the elements of the methodical approach will be described in detail.

3.1 Efficiency Maps of Electrical Machines

In HEV system-level design optimization, electrical machines are usually modeled as efficiency maps of the form $\eta_{EM}(T_{EM}, \omega_{EM})$, as it is plotted in Figure 4.
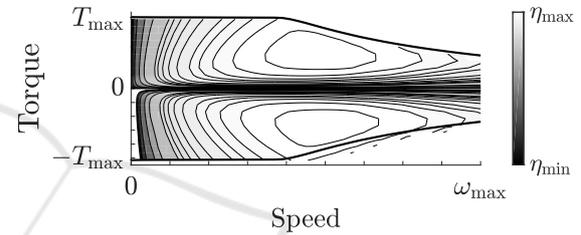

Figure 4: Example of an EM efficiency map.

In this diagram, the torque limitations are represented by the bold lines for motoring $T_{EM,max}$ and generating $-T_{EM,max}$. The efficiencies are given by the isolines within the maximum torque curves and calculated as the ratio of the mechanical power output $P_{EM,mech}$ and the electrical power input $P_{EM,el}$:

$$\eta_{EM} = \begin{cases} \dfrac{P_{EM,mech}}{P_{EM,el}} & \text{for } P_{EM,mech} > 0 \text{ (mot.)} \\ \dfrac{P_{EM,el}}{P_{EM,mech}} & \text{for } P_{EM,mech} < 0 \text{ (gen.)} \end{cases} \quad (2)$$

As it can be seen from the formulation above, the calculation of the efficiency maps differs for motoring and generating. In this work, $P_{EM,el}$ describes the power either drawn from or supplied to the battery of the HEV. The approximation of the efficiency behavior can become a challenging task especially in areas close to the origin axes, since the efficiency is not defined within this regions. Thus, a pragmatic approach is to carry out first the approximation of the electrical power map $P_{EM,el}(T_{EM}, \omega_{EM})$ and then second the calculation of η_{EM} by the definition given in (2).

3.2 Database and Design Space

The models in this approach consider all losses within the electrical and mechanical path, e.g., the EM's iron

losses, copper losses and friction losses, as well as losses caused by power electronics (PE) and thus represent the whole EM system.

3.2.1 FEA Model Database

In order to allow the consideration of possible EM system designs over a wide design range with suitable accuracy, the training data is based on highly accurate simulation models. In this work, an analytical scaling procedure is applied to a set of FEA models, where each FEA model represents an EM with a specific active diameter d_{EM}. The analytical scaling along the design dimensions length l_{EM} and number of turns per coil TC_{EM} allows one to consider EMs spread over the whole design space within the training data. In this work, only permanent magnet synchronous motors (PMSM) are considered. Furthermore, the technology of these machines is identical in terms of e.g., magnet layout, winding diagram etc to represent an unbiased data set. The design space to be covered by the MLP-based SEMM is defined by the continuous geometrical EM parameters active diameter and length as well as the discrete number of turns per coil. Each design within the database refers to an efficiency optimized EM system including the electrical machine and its corresponding PE and is characterized by its specific efficiency map (see (2)) and its maximum torque curves. Due to the definition of continuous design variables, the theoretical number of possible EM designs is infinite.

3.2.2 Design of Experiments

Since the efficiency maps of each machine design are based on a large number of torque and speed combinations, the computational effort of the training process increases with the number of considered machine designs.
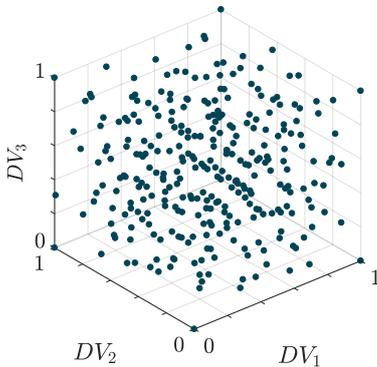

Figure 5: Illustration of a Sobol design with three design variables and 300 electrical machine designs.

Furthermore, the more designs are considered, the more time-consuming simulations are required for the generation of the training data. Due to the high computational effort of the FEA simulations based data generation and in order to realize a practicable methodology for the development of scalable EM models, a DoE approach is applied to reduce the number of considered designs while maintaining a sufficient amount of data for the MLP training. Therefore, a Sobol distributed spacefilling design (cf. (Santner et al., 2003)) is used for the choice of a suitable amount of informative training data within the design space. For clarity, Figure 5 illustrates a Sobol design with three design variables (DV_i) defined on the normalized interval $[0,1]$. Within this work, the variables d_{EM}, l_{EM} and TC_{EM} span a 3 dimensional design space over specific variable ranges.

3.3 Scalable Electrical Machine Model

The characteristics of single EM design are defined by their efficiency maps and the maximum torque curves and therefore, the two separated models $\hat{y}_{Con}$ and $\hat{y}_{Lim}$ are used for the approximation of the electrical power consumption map and the torque limitations respectively. The scalability of the models is given by the consideration of different EM designs an the interpolation capability of the MLP.

3.3.1 Training Data

The training data is based on 300 EM designs defined by the design parameters d_{EM}, l_{EM} and TC_{EM} where each design refers to a torque-speed-grid with several thousand sample points.
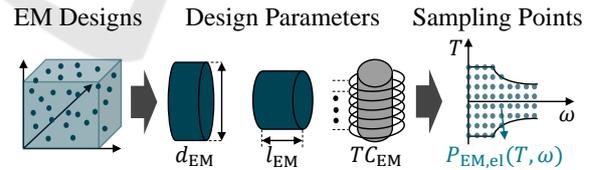

Figure 6: Schematic of the training data composition.

Figure 6 illustrates schematically the generation and composition of the training data for the training process. The target y_{Con} for the training process of $\hat{y}_{Con}$ is defined by the electrical power $P_{EM,el}$ of the EM systems at each sample point of the torque-speed-grids. Thus, the input training data of a single machine design is represented by the matrix

$$\underline{U}_{Con,i} = \begin{bmatrix} d_{EM,i} & d_{EM,i} & \dots & d_{EM,i} \\ l_{EM,i} & l_{EM,i} & \dots & l_{EM,i} \\ TC_{EM,i} & TC_{EM,i} & \dots & TC_{EM,i} \\ T_{EM,i,1} & T_{EM,i,2} & \dots & T_{EM,i,N_C} \\ \omega_{EM,i,1} & \omega_{EM,i,2} & \dots & \omega_{EM,i,N_C} \end{bmatrix}, \quad (3)$$

where N_C denotes the number of torque-speed-combinations of a single EM. Thus, the entire training data set for M machine designs is given by:

$$\underline{U}_{\text{Con}} = [\underline{U}_{\text{Con},1} \ \underline{U}_{\text{Con},2} \ \cdots \ \underline{U}_{\text{Con},M}] \qquad (4)$$

According to the schematic in Figure 6 and in analogy to the formulations of (3) and (4) the target data of a single machine design is given by the vector

$$\underline{y}_{\text{Con},i} = [P_{\text{EM,el},i,1} \ P_{\text{EM,el},i,2} \ \cdots \ P_{\text{EM,el},i,N_C}], \qquad (5)$$

and the entire target data is represented by:

$$\underline{y}_{\text{Con}} = [\underline{y}_{\text{Con},1}, \underline{y}_{\text{Con},2}, \cdots, \underline{y}_{\text{Con},M}] \qquad (6)$$

Furthermore, the respective vectors of speed values $\underline{\omega}_{\text{EM},i} = [\omega_{\text{EM},i,1} \ \omega_{\text{EM},i,2} \ \cdots \ \omega_{\text{EM},i,N_S}]$ and the corresponding vectors of maximum torque values $\underline{T}_{\text{EM,max},i} = [T_{\text{EM,max},i,1} \ T_{\text{EM,max},i,2} \ \cdots \ T_{\text{EM,max},i,N_S}]$ with N_S elements are used for the training of the scalable torque limitation model $\hat{y}_{\text{Lim}}$:

$$\underline{U}_{\text{Lim}} = [\underline{U}_{\text{Lim},1} \ \underline{U}_{\text{Lim},2} \ \cdots \ \underline{U}_{\text{Lim},M}] \qquad (7)$$

$$\underline{y}_{\text{Lim}} = [\underline{T}_{\text{EM,max},1} \ \underline{T}_{\text{EM,max},2} \ \cdots \ \underline{T}_{\text{EM,max},M}] \qquad (8)$$

In analogy to 3, the first three rows of the matrices $\underline{U}_{\text{lim},i}$ in 7 are the corresponding values of the design variables of the i-th machine design.

3.3.2 Training Process

In this work, a nonlinear optimization of the weights and biases is carried out by the Levenberg-Marquard algorithm (Marquardt, 1963) to minimize the sum squared errors of the two models. The used optimization technique speeds up the training convergence compared to the standard gradient descend backpropagation algorithm (Hagan and Menhaj, 1994). Furthermore, the training convergence depends on a suitable initialization of weights and biases. Thus, a widely accepted approach based on statistical analysis for controlled activation weight initialization (Drago and Ridella, 1992) is applied within this paper. The attributes of the utilized MLPs are shown in Table 1:

Table 1: Attributes of the utilized models.

Model	Structure	σ	Objective
$\hat{y}_{\text{Con}}$	5-80-1	tanh	SSE
$\hat{y}_{\text{Lim}}$	4-12-12-1	tanh	SSE

Both models use hyperbolic tangent (tanh) as activation function and are trained by the minimization of the sum-squared-error

$$SSE_{\text{U}} = \sum_{m=1}^{N_{\text{tr}}} (y(m) - \hat{y}(m))^2, \qquad (9)$$

where N_{tr} denotes the length of the respective training data set. The model structure is given by a structure code, where the first number refers to the number of inputs, the last number refers to the number of outputs and the remaining numbers refer to the respective number of hidden layer neurons. The structure of the MLPs in this work is found by iteratively increasing the number of hidden layer neurons until the model accuracy requirements are met (bias-variance tradeoff, see (Winsel, 2002)). In case the potential of accuracy improvement is exhausted prior the requirements are met, an additional hidden layer is used and the procedure is repeated. Thus, the consumption model $\hat{y}_{\text{Con}}$ was found as a three layer network with 5 inputs, one hidden layer with 80 neurons and 1 output. For an accurate approximation of the constant torque characteristics, 2 hidden layers have shown a better performance and thus are used in this work within the limitation model $\hat{y}_{\text{Lim}}$.

3.4 Model Validation

The validation of the models is split into two steps and illustrated schematically in Figure 7. The first step is carried out during the training process by dividing the data set into a training set and a validation set consisting of speed-torque combinations and the corresponding electrical power values.
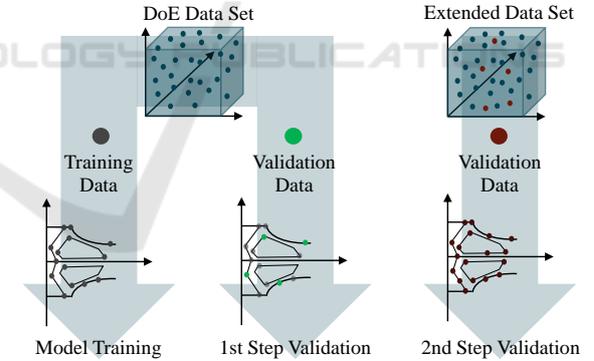

Figure 7: Schematic illustration of the model validation.

Thus, an amount of 20 % of the data points is used to validate the model performance within the electrical power maps of each EM existent in the training data by applying the statistics $RMSE_{\text{val}}$ given by

$$RMSE_{\text{val}} = \sqrt{\frac{1}{N_{\text{val}}} SSE_{\text{val}}}, \qquad (10)$$

and coefficient of determination R^2_{val}

$$R^2_{\text{val}} = 1 - \frac{SSE_{\text{val}}}{\sum_{m=1}^{N_{\text{val}}} (y(m) - \bar{y})^2}, \qquad (11)$$

as a measure of the goodness of the model fit (Magee, 1990), where $\bar{y}$ denotes the mean of the output values. These statistics are also used within the second step of model validation. Therefore, an additional data set consisting of EM designs not included within the training data is used for the validation of the interpolation behavior of the scalable models. In this context, the goodness of interpolation behavior is defined by the extent of overfitting or underfitting within the model. Figure 8 shows the distribution of 60 EM designs as they are used for the second step of model validation.
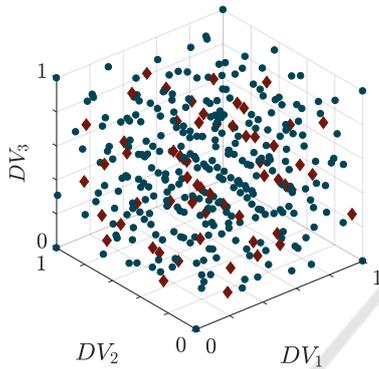

Figure 8: Distribution of additional EM designs for model validation.

The EM designs for the validation (red diamonds) are given by an extension of the original Sobol distribution and the data is generated by following the data generation procedure described in Section 3.2 for the additional designs.

4 RESULTS

In this section, the introduced methodology is applied on the defined FEA simulation based training data set and verified by an exemplary analysis of the training convergence and the resulting model error of the consumption model $\hat{y}_{Con}$. With respect to the application field in HEV system-level design, a simulation study is carried out to prove the model performance within a practical context.

4.1 Model Analysis

The verification of the model performance is carried out during the model training and shown in Figure 9. In diagram a), the minimization progress of the *RMSE* is plotted against the number of iterations. Considering R^2 on its defined co-domain $[0, 1]$, val-

ues close to 1 represent a good model fit if the training data is not affected with measurement uncertainty. Since the progress of R^2 converges to 1, the trained model achieves the required performance.

(a) *RMSE*

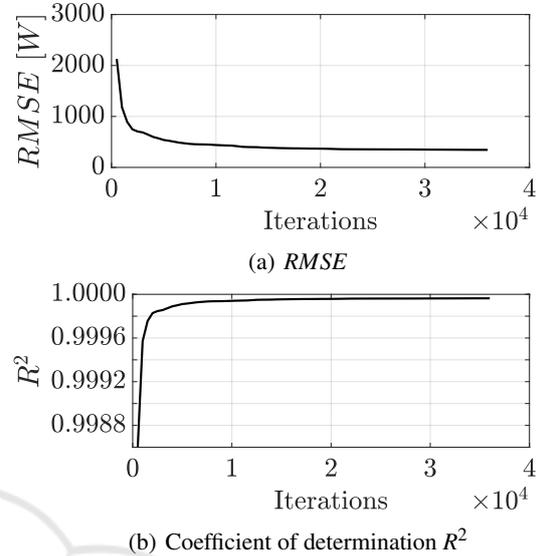(b) Coefficient of determination R^2

Figure 9: Training convergence and model verification.

The success of the training is summarized for the consumption model $\hat{y}_{Con}$ and the limitation model $\hat{y}_{Lim}$ by the resulting statistics given in Table 2:

Table 2: Resulting tranining statistics.

Statistic	$\hat{y}_{Con}$	$\hat{y}_{Lim}$
RMSE	344 W	2.85 Nm
R^2	0.999963479	0.999593949

Furthermore, the validation confirms the goodness of the model fit with similar statistics as achieved during the verification process. These measures are given for both models and two validation steps in Table 3

Table 3: Resulting validation statistics.

Statistic	$\hat{y}_{Con}$	$\hat{y}_{Lim}$
$RMSE_{val,1}$	345 W	2.85 Nm
$R^2_{val,1}$	0.999963305	0.999597185
$RMSE_{val,2}$	324 W	2.87 Nm
$R^2_{val,2}$	0.999967438	0.999569435

Due to the application field in HEV system-level design, the scalable EM models require rather high values of R^2 than in other modeling tasks since small deviations in electrical power maps can lead to significant differences within the evaluation of energy consumption. For example an model error of 10 W does not significantly affect the evaluation of energy consumption at high loads e.g., 100 kW, but does in areas of small loads as it is present in typical driving cycles.

4.2 Simulation Study

In order to prove the practicality of the developed MLP-based scalable EM models, an exemplary simulation study is carried out. Thereby, the operating points of the EM in electric drive mode for specific HEV topologies are used for the evaluation of the electrical energy consumption. These operating points are drawn from a hybrid vehicle simulation model and refer to the Worldwide Harmonized Light Vehicles Test Procedure (WLTP). Figure 10 illustrates the operating points plotted into the efficiency maps of an exemplary FEA based model a) and the corresponding MLP model b) for a specific EM design.
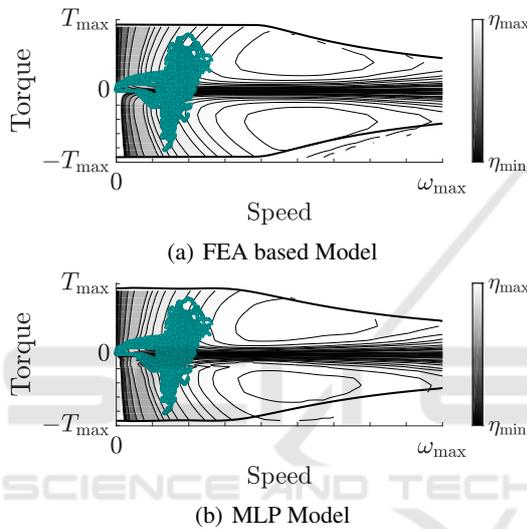

(a) FEA based Model

(b) MLP Model

Figure 10: Efficiency maps with WLPT operating points.

The qualitative comparison of the map characteristics shows notably deviations in areas close to zero torque and close to the torque limitation curves. This behavior was observed for a wide range within the considered design space. In order to quantitatively asses the deviations significance in means of energy consumption evaluation, 5 EM designs (including designs not represented within the training data) are varied within 3 different HEV topologies and thus are evaluated at different operating points.

Table 4: Relative deviations of energy consumption.

Variations	Top 1	Top 2	Top 3
EM_1	0.131 %	0.691 %	0.867 %
EM_2	0.387 %	1.048 %	0.143 %
EM_3	2.662 %	2.202 %	1.480 %
EM_4	0.404 %	1.004 %	0.226 %
EM_5	1.153 %	0.553 %	0.169 %

The relative deviations of the MLP models electrical energy consumptions are given in Table 4. The

investigated electrical machine EM_3 is conspicuous because of a rather high relative deviation compared to the remaining values. In this case, EM_3 is characterized by a high maximum torque and thus oversized with respect to the WLTP operating points. Keeping this fact in mind, significant deviation can be overcome by an adequate setting of the design variable limits. Since the deviations of the remaining EM designs mostly show values smaller than 1 %, the scalable EM models possesses sufficient accuracy and saving potential in terms of computation time if more than 1800 simulations are carried out (see Fig. 11).
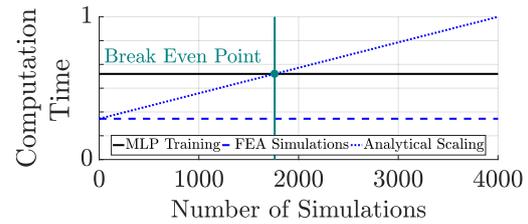

Figure 11: Break even point of simulation numbers.

The diagram shown above can be adapted to arbitrary data generation procedures to assess the efficiency of the proposed modelling approach.

5 CONCLUSIONS

The main focus of this research is a methodical approach using the strength of Neural Networks in nonlinear function approximation for the development of scalable EM models. This work is motivated by typical requirements in HEV system-level design optimization in terms of component modeling, namely scalability and the achievement of sufficient accuracy with practicable computational effort.

The MLP-based scalable EM models developed in this paper are capable to represent the characteristics of each EM design within the given design space. Thus, once the model is trained, it can be directly implemented and used within typical HEV system-level design simulation studies, e.g., component sizing, by varying the specified design variables. Since only a small number of FEA simulations and analytical scaling procedures must be performed uniquely, the introduced approach benefits from high saving potential in terms of computational effort. The MLP model's performance is validated by a statistical analysis and its practicality is proven within an application example. Future work will include research on different optimization targets, e.g., single losses of the EM system, and network structures to further increase the model performance.

REFERENCES

Buecherl, D., Bertram, C., Thanheiser, A., and Herzog, H.-G. (2010). Scalability as a degree of freedom in electric drive train simulation. In *2010 IEEE Vehicle Power and Propulsion Conference*. IEEE.

Domingues, G., Reinap, A., and Alakula, M. (2016). Design and cost optimization of electrified automotive powertrain. In *2016 International Conference on Electrical Systems for Aircraft, Railway, Ship Propulsion and Road Vehicles & International Transportation Electrification Conference (ESARS-ITEC)*. IEEE.

Drago, G. and Ridella, S. (1992). Statistically controlled activation weight initialization (SCAWI). *IEEE Transactions on Neural Networks*, 3(4):627–631.

Gao, W. and Porandla, S. (2005). Design optimization of a parallel hybrid electric powertrain. In *2005 IEEE Vehicle Power and Propulsion Conference*. IEEE.

Hagan, M. and Menhaj, M. (1994). Training feedforward networks with the marquardt algorithm. *IEEE Transactions on Neural Networks*, 5(6):989–993.

Hofman, T., Ebbesen, S., and Guzzella, L. (2012). Topology optimization for hybrid electric vehicles with automated transmissions. *IEEE Transactions on Vehicular Technology*, 61(6):2442–2451.

Hornik, K., Stinchcombe, M., and White, H. (1989). Multilayer feedforward networks are universal approximators. *Neural Networks*, 2(5):359–366.

Magee, L. (1990). R2measures based on wald and likelihood ratio joint significance tests. *The American Statistician*, 44(3):250–253.

Marquardt, D. W. (1963). An algorithm for least-squares estimation of nonlinear parameters. *Journal of the Society for Industrial and Applied Mathematics*, 11(2):431–441.

Nelles, O. (2001). *Nonlinear System Identification*. Springer Berlin Heidelberg.

Rumelhart, D. E., Hinton, G. E., and Williams, R. J. (1986). Learning representations by back-propagating errors. *Nature*, 323(6088):533–536.

Santner, T. J., Williams, B. J., and Notz, W. I. (2003). *The Design and Analysis of Computer Experiments*. Springer New York.

Silvas, E., Hofman, T., Murgovski, N., Etman, P., and Steinbuch, M. (2016). Review of optimization strategies for system-level design in hybrid electric vehicles. *IEEE Transactions on Vehicular Technology*, pages 1–1.

Stipetic, S. and Goss, J. (2016). Calculation of efficiency maps using scalable saturated flux-linkage and loss model of a synchronous motor. In *2016 XXII International Conference on Electrical Machines (ICEM)*. IEEE.

Vaillant, M. (2016). *Design Space Exploration zur multikriteriellen Optimierung elektrischer Sportwagenantriebsstränge: Variation von Topologie und Komponenteneigenschaften zur Steigerung von Fahrleistungen und Tank-to-Wheel Wirkungsgrad*. PhD thesis, KIT Karlsruhe.

Winsel, T. (2002). *Stabile neuronale Prozessmodelle - automatisierte Generierung echtzeitfhiger Modelle zur Nachbildung des dynamischen Verhaltens von Verbrennungsmotoren*. VDI-Verlag, Dsseldorf.

Wirasingha, S. G. and Emadi, A. (2011). Classification and review of control strategies for plug-in hybrid electric vehicles. *IEEE Transactions on Vehicular Technology*, 60(1):111–122.

Zhou, K., Ivanco, A., Filipi, Z., and Hofmann, H. (2015). Finite-element-based computationally efficient scalable electric machine model suitable for electrified powertrain simulation and optimization. *IEEE Transactions on Industry Applications*, 51(6):4435–4445.